

Proton-Coupled Electron-Transfer Reactions. Mechanisms of Two-Electron Reduction of *trans*-Dioxoruthenium(VI) to *trans*-Aquooxoruthenium(VI) and Disproportionation of *trans*-Dioxoruthenium(V)

Chi-Ming Che,^{*,1a} Keung Lau,^{1a} Tai-Chu Lau,^{1a,b} and Chung-Kwong Poon^{1a}

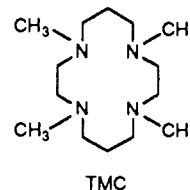
Contribution from the Department of Chemistry, University of Hong Kong, Pokfulam Road, Hong Kong. Received January 10, 1989. Revised Manuscript Received February 26, 1990

Abstract: The kinetics and mechanism of the reduction of *trans*-[Ru^{VI}(TMC)(O)₂]²⁺ to *trans*-[Ru^{IV}(TMC)O(H₂O)]²⁺ (TMC = 1,4,8,11-tetramethyl-1,4,8,11-tetraazacyclotetradecane) in aqueous solution by outer-sphere one-electron reductants (R), *trans*-[Ru^{VI}(TMC)(O)₂]²⁺ + 2R + 2H⁺ → *trans*-[Ru^{IV}(TMC)O(H₂O)]²⁺ + 2R⁺, have been studied. The first step of the reduction is a simple outer-sphere electron-transfer process, *trans*-[Ru^{VI}(TMC)(O)₂]²⁺ + R → *trans*-[Ru^V(TMC)(O)₂]⁺ + R⁺ with rate = *k*₂[Ru(VI)][R]. The rate constants (*k*₂) with *cis*-[Ru^{II}(NH₃)₄bpy]²⁺ (bpy = 2,2'-bipyridine), [Ru^{II}(NH₃)₃isn]²⁺ (isn = isonicotinamide), and [Ru^{II}(NH₃)₃py]²⁺ (py = pyridine) have been measured and can be correlated with the Marcus cross relation. The estimated self-exchange rate constant of the *trans*-[Ru^{VI}(TMC)(O)₂]²⁺/*trans*-[Ru^V(TMC)(O)₂]⁺ couple is 1.5 × 10⁵ mol⁻¹ dm³ s⁻¹ (*I* = 0.1 M) at 298 K. When *trans*-[Ru^{VI}(TMC)(O)₂]²⁺ is in excess, the *trans*-[Ru^V(TMC)(O)₂]⁺ species formed will undergo rapid disproportionation, 2*trans*-[Ru^V(TMC)(O)₂]⁺ + 2H⁺ → *trans*-[Ru^{VI}(TMC)(O)₂]²⁺ + *trans*-[Ru^{IV}(TMC)O(H₂O)]²⁺. The disproportionation follows the rate law: rate = *k*_{dis}[Ru(V)]² with *k*_{dis} = 2*k*_e*K*_p[H⁺]/(1 + *K*_p[H⁺])². The *K*_p and *k*_e are referred to the equilibrium constant and rate constant for the respective reactions, *trans*-[Ru^V(TMC)(O)₂]⁺ + H⁺ ⇌ *trans*-[Ru^V(TMC)O(OH)]²⁺ and *trans*-[Ru^V(TMC)O(OH)]²⁺ + *trans*-[Ru^V(TMC)(O)₂]⁺ → *trans*-[Ru^{VI}(TMC)(O)₂]²⁺ + *trans*-[Ru^{IV}(TMC)O(OH)]²⁺. At 299 K and *I* = 0.1 M, *K*_p and *k*_e have been determined to be 615 ± 50 mol⁻¹ dm³ and (2.72 ± 0.34) × 10⁶ mol⁻¹ dm³ s⁻¹, respectively. The self-exchange rate constant of the *trans*-[Ru^V(TMC)O(OH)]²⁺/*trans*-[Ru^{IV}(TMC)O(OH)]²⁺ has been estimated to be 5 × 10³ mol⁻¹ dm³ s⁻¹ at 298 K and *I* = 0.1 M.

Oxo complexes of ruthenium(VI), ruthenium(V), and ruthenium(IV) have received much attention in recent years because of their remarkable abilities as stoichiometric and catalytic oxidants.²⁻⁷ Among the various oxoruthenium species, the Ru(IV)-oxo complex [Ru^{IV}(bpy)₂(py)O]²⁺ (bpy = 2,2'-bipyridine; py = pyridine) has been extensively studied by Meyer and co-workers.³ Oxidation by this complex can proceed through a variety of pathways including oxygen-atom transfer, hydrogen-atom, and

hydride transfer. In contrast, although a number of *trans*-dioxoruthenium(VI) species have been synthesized and shown to be good oxidants for quite some time,^{2c-1,4,5,7} relatively few mechanistic details are known.^{2k} We have thus initiated a program to study the reactions of *trans*-dioxoruthenium(VI) complexes with various inorganic and organic substrates in order to find out the various mechanistic pathways and the factors determining which pathway would be preferred in a given reaction. Our interest in the redox chemistry of *trans*-dioxoruthenium(VI) also arises as a result of previous electrochemical studies,^{8,9} indicating that this class of compounds are potent electrooxidative catalysts and exhibit reversible dioxoruthenium(VI)/oxo-aquo-ruthenium(IV) couple in aqueous solution. The reversible M=O/M—OH₂ redox couple, which has not been encountered with the classical metal-oxo oxidants such as MnO₄⁻ and CrO₄²⁻, is commonly observed in the electrochemistry of ruthenium and osmium oxo complexes.^{3f,8,10}

We report here the results of a rate and mechanistic study on the reaction of *trans*-[Ru^{VI}(TMC)(O)₂]²⁺,^{2c} (TMC = 1,4,8,11-tetramethyl-1,4,8,11-tetraazacyclotetradecane) with some simple outer-sphere reductants: *cis*-[Ru^{II}(NH₃)₄bpy]²⁺, [Ru^{II}(NH₃)₃isn]²⁺ (isn = isonicotinamide), and [Ru^{II}(NH₃)₃py]²⁺. The goal of this work is to obtain detailed kinetic, thermodynamic, and mechanistic information about the reduction of Ru(VI) to Ru(IV). The TMC system is particularly attractive for use in



- (1) (a) Department of Chemistry, University of Hong Kong, Pokfulam Road, Hong Kong. (b) Present address: Department of Applied Science, City Polytechnic of Hong Kong, Tat Chee Avenue, Kowloon Tong, Hong Kong.
- (2) (a) Che, C. M.; Wong, K. Y.; Mak, T. C. W. *J. Chem. Soc., Chem. Commun.* **1985**, 988. (b) Che, C. M.; Wong, K. Y.; Mak, T. C. W. *J. Chem. Soc., Chem. Commun.* **1985**, 988. (c) Che, C. M.; Wong, K. Y.; Poon, C. K. *Inorg. Chem.* **1985**, *24*, 1797. (d) Che, C. M.; Wong, K. Y. *J. Chem. Soc., Chem. Commun.* **1986**, 22. (e) Che, C. M.; Wong, K. Y.; Leung, W. H.; Poon, C. K. *Inorg. Chem.* **1986**, *25*, 345. (f) Che, C. M.; Lai, T. F.; Wong, K. Y. *Inorg. Chem.* **1987**, *22*, 2289. (g) Che, C. M.; Leung, W. H. *J. Chem. Soc., Chem. Commun.* **1987**, 1376. (h) Che, C. M.; Tang, W. T.; Wong, W. T.; Lai, T. F. *J. Am. Chem. Soc.* **1989**, *111*, 9048. (i) Leung, W. H.; Che, C. M. *J. Am. Chem. Soc.* **1989**, *111*, 8812. (j) Che, C. M.; Tang, W. T.; Wong, W. T.; Lai, T. F. *J. Chem. Soc., Dalton Trans.* **1989**, 2011. (k) Che, C. M.; Wong, K. Y. *J. Chem. Soc., Dalton Trans.* **1989**, 2065.
- (3) Recent works by Meyer and co-worker: (a) Dobson, J. C.; Seok, W. K.; Meyer, T. J. *Inorg. Chem.* **1986**, *25*, 1514. (b) Binstead, R. A.; Meyer, T. J. *J. Am. Chem. Soc.* **1987**, *109*, 3287. (c) Gilbert, J.; Roecker, L.; Meyer, T. J. *Inorg. Chem.* **1987**, *26*, 1126. (d) Roecker, L.; Meyer, T. J. *J. Am. Chem. Soc.* **1987**, *109*, 746. (e) Seok, W. K.; Dobson, J. C.; Meyer, T. J. *Inorg. Chem.* **1988**, *27*, 5. (f) Dobson, J. C.; Meyer, T. J. *Inorg. Chem.* **1988**, *27*, 3283.
- (4) (a) Griffith, W. P.; Pawson, D. *J. Chem. Soc., Dalton Trans.* **1973**, 1316. (b) Schroder, M.; Griffith, W. P. *J. Chem. Soc., Chem. Commun.* **1979**, 68. (c) Green, G.; Griffith, W. P.; Hollinshead, D. M.; Ley, S. V.; Schroder, M. *J. Chem. Soc., Perkin Trans. 1* **1984**, 681. (d) Griffith, W. P.; Ley, S. V.; White, A. D. *J. Chem. Soc., Chem. Commun.* **1987**, 1625. (e) El-Hendawy, A. M.; Griffith, W. P.; Piggot, B.; Williams, D. J. *J. Chem. Soc., Dalton Trans.* **1988**, 1983.
- (5) (a) Groves, J. T.; Quinn, R. *Inorg. Chem.* **1984**, *23*, 3844. (b) Groves, J. T.; Quinn, R. *J. Am. Chem. Soc.* **1985**, *107*, 5790. (c) Groves, J. T.; Ahn, K. H. *Inorg. Chem.* **1987**, *26*, 3833.
- (6) (a) Marmion, M. E.; Takeuchi, K. *J. Am. Chem. Soc.* **1986**, *108*, 510. (b) Marmion, M. E.; Takeuchi, K. *J. Am. Chem. Soc.* **1988**, *110*, 1472.
- (7) Lau, T. C.; Kochi, J. K. *J. Chem. Soc., Chem. Commun.* **1987**, 179.

- (8) Che, C. M.; Wong, K. Y.; Anson, F. C. *J. Electroanal. Chem.* **1987**, *226*, 211.
- (9) Che, C. M.; Leung, W. H.; Poon, C. K. *J. Chem. Soc., Chem. Commun.* **1987**, 173.
- (10) (a) Pipes, D. W.; Meyer, T. J. *J. Am. Chem. Soc.* **1984**, *106*, 7653. (b) Che, C. M.; Cheng, W. K. *J. Am. Chem. Soc.* **1986**, *108*, 4644.

this study for the following reasons: (1) *trans*-[Ru^{VI}(TMC)(O)₂]²⁺ is stable to decomposition and (2) possible intermediates and products such as *trans*-[Ru^V(TMC)(O)₂]⁺ and *trans*-[Ru^{IV}(TMC)O(OH₂)]²⁺ have been well-characterized,^{2f} thus making mechanistic study relatively easy.

Experimental Section

Materials. *trans*-[Ru^{VI}(TMC)(O)₂](PF₆)₂,^{2c} *cis*-[Ru^{II}(NH₃)₄bpy](PF₆)₂,¹¹ [Ru^{II}(NH₃)₅py](PF₆)₂,¹² and [Ru^{II}(NH₃)₅isn](PF₆)₂¹² were prepared by literature methods. Water used for kinetic experiments was distilled twice from potassium permanganate.

Trifluoromethanesulfonic acid (Aldrich), monochloroacetic acid, acetic acid, and sodium hydroxide were used to maintain pH. Sodium trifluoromethanesulfonate (made by neutralizing trifluoromethanesulfonic acid with sodium hydroxide) was used to maintain ionic strength. D₂O (99.9% D, Aldrich), CD₃COOD (99.9% D, Merck), and DClO₄ (99.8% D, Merck) were used as received.

Kinetic Measurements. Routine UV-vis spectra were obtained with a Shimadzu UV-240 spectrophotometer. Kinetic measurements were made with a Hi-Tech SF-51 stopped-flow module coupled with a Hi-Tech SU-40 spectrophotometric unit. The data collection process was controlled by an Apple IIe microcomputer via an ADS-1 interface unit, also from Hi-Tech.

The reaction between Ru(VI) and Ru(II) was found to occur in two stages: a rapid reduction of Ru(VI) to Ru(V) followed by a slower disproportionation of Ru(V) (see results). Under the condition that the concentration of Ru(VI) is in 10-fold excess of the Ru(II) reductant ([Ru(VI)] = 5 × 10⁻⁵–5 × 10⁻⁴ M, [Ru(II)] = 5 × 10⁻⁶–5 × 10⁻⁵ M), the kinetics of the first step was followed by monitoring the MLCT band of the Ru(II) complex (*cis*-[Ru^{II}(NH₃)₄bpy]²⁺, 522 nm; [Ru^{II}(NH₃)₅py]²⁺, 475 nm; [Ru^{II}(NH₃)₅isn]²⁺, 478 nm). Pseudo-first-order rate constants, *k*_{obs}, were obtained by nonlinear least-squares fits^{13,14} of *A*_{*t*} to time *t* according to the equation *A*_{*t*} = *A*_∞ + (*A*₀ - *A*_∞) exp(-*k*_{obs}*t*), where *A*₀ and *A*_∞ are the initial and final absorbances, respectively. Second-order rate constants, *k*₂, were obtained from linear least-square fits of *k*_{obs} to [Ru(VI)].

The second stage of the reaction, i.e., disproportionation of Ru(V), was followed at 300 nm (near λ_{max} of Ru(V) in CH₃CN).^{2d} In most runs concentrations of reactants were higher ([Ru(VI)] = 3 × 10⁻⁴–1 × 10⁻³ M, [Ru(II)] = 5 × 10⁻⁵–2 × 10⁻⁴ M) than that used in studying the first stage of the reaction in order to obtain a large enough absorbance change and to ensure that the first stage is fast enough as not to interfere with the second stage. In other words, separate experiments were performed, in most cases, to follow the two stages of the reaction. The order of the disproportionation was determined by using Wilkinson's equation¹⁴

$$\frac{t}{p} = \frac{nt}{2} + \frac{1}{K} \quad (1)$$

where *p* = 1 - *C*_{*t*}/*C*₀, the fraction reacted, *n* = order of the reaction, and *K* = *k*_{dis}*C*₀^{*n*-1}. *k*_{dis} is the disproportionation rate constant. *C*₀ is the initial concentration of Ru(V) ([Ru(V)]₀) and is proportional to (*A*₀ - *A*_∞). *C*_{*t*} is the concentration of Ru(V) at time *t* ([Ru(V)]_{*t*}) and is proportional to (*A*_{*t*} - *A*_∞). Equation 1 can thus be written as

$$\frac{t}{p} = \frac{t(A_0 - A_\infty)}{(A_0 - A_t)} = \frac{nt}{2} + \frac{1}{k_{\text{dis}}[\text{Ru(V)}]_0^{n-1}} \quad (2)$$

Equation 2 was used to verify that the reaction is second order and to obtain an approximate value of *k*_{dis}. Equation 2 can be rearranged to eq 3, by using *n* = 2

$$A_t = \alpha / (1 + \tau t) + \beta \quad (3)$$

where

$$\alpha = A_0 - A_\infty$$

$$\beta = A_\infty$$

$$\tau = [\text{Ru(V)}]_0 k_{\text{dis}}$$

The value of *k*_{dis} was refined by a nonlinear least-squares fit¹³ of absorbance *A*_{*t*} to time *t* according to eq 3, taking the concentration of

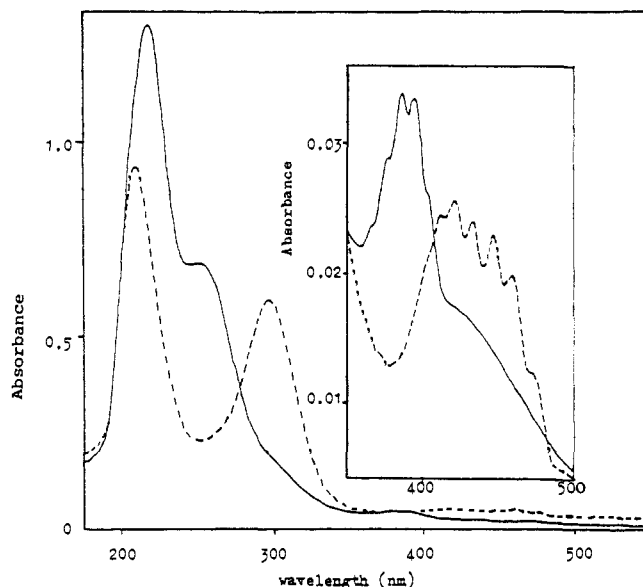
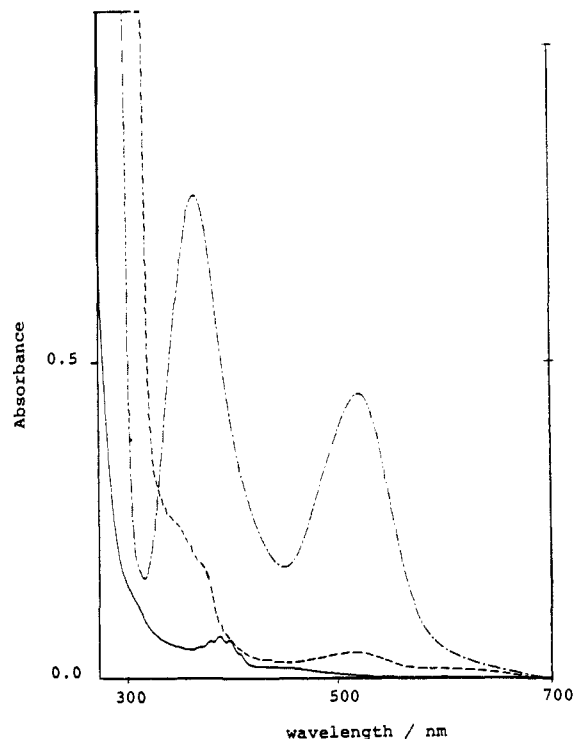


Figure 1. (a) UV-vis spectral changes for the reaction between *trans*-[Ru^{VI}(TMC)(O)₂]²⁺ (0.8 × 10⁻⁴ M) and *cis*-[Ru^{II}(NH₃)₄bpy]²⁺ (1.6 × 10⁻⁴ M) in 0.1 M CF₃SO₃H: Ru(VI), (—); Ru(II), (---); and final spectrum, (-·-). (b) UV-vis spectral changes for the reaction between *trans*-[Ru^V(TMC)(O)₂]⁺ (~1 × 10⁻⁴ M) and 5 equiv of CF₃COOH in acetonitrile. The final spectrum (—) is identical with that of an acetonitrile solution containing equal concentrations of *trans*-[Ru^{VI}(TMC)(O)₂]²⁺ and *trans*-[Ru^{IV}(TMC)O(CH₃CN)]²⁺.

Ru(II) used as [Ru(V)]₀ and using α, β, and τ as adjustable parameters.

Product and Stoichiometry. The stoichiometry for the *cis*-[Ru^{II}(NH₃)₄bpy]²⁺ reduction of *trans*-[Ru^{VI}(TMC)(O)₂]²⁺ in 0.1 M was determined by adding various amounts of Ru(II) to Ru(VI) (initially present in excess) and monitoring absorbance changes at 522 nm (λ_{max} of Ru(II)). A stoichiometry of 2Ru(II):1Ru(VI) was obtained from the plot of absorbance vs [Ru(II)]/[Ru(VI)] (Figure S1, Supplementary Material). Determination of the reaction stoichiometry under the condition that [Ru(VI)] is in 5-fold excess of [Ru(II)] has also been attempted. The amount of *trans*-[Ru^{IV}(TMC)O(OH₂O)]²⁺ formed was estimated by measuring the absorbance change at 420 nm where the Ru(VI) species does not have any absorption. The result obtained is similar to that described above but is less accurate because of the low ε_{max} (150 mol⁻¹ dm³ cm⁻¹) of Ru(IV) at this wavelength. The product resulting from the reduction of Ru(VI) was determined as follows. Typ-

(11) Alvarez, V. E.; Allen, R. J.; Matsubara, T.; Ford, P. C. *J. Am. Chem. Soc.* **1974**, *96*, 7686.

(12) Gaunder, R. G.; Taube, H. *Inorg. Chem.* **1970**, *9*, 2627.

(13) The nonlinear least-squares programs used in this study were written in Apple Soft Basic and run on Apple IIe under the PRODOS environment. Lau, K. Ph.D. Thesis, University of Hong Kong, 1988.

(14) Moore, J. W.; Pearson, R. G. *Kinetics and Mechanism*; Wiley: New York, 1981; p 21.

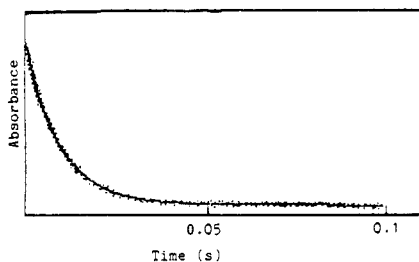
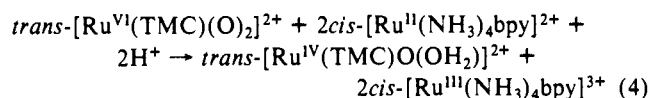


Figure 2. Absorbance vs time output of the nonlinear least-squares program for the reduction of $trans\text{-}[Ru^{VI}(TMC)(O)_2]^{2+}$ (2×10^{-4} M) by $cis\text{-}[Ru^{II}(NH_3)_4bpy]^{2+}$ (2×10^{-5} M) at 522 nm, $T = 292.7$ K, $I = 0.01$ M: dotted line, experimental data; solid line, theoretical curve.

ically 1.07×10^{-6} mol of Ru(VI) was mixed with 2.17×10^{-6} mol of Ru(II) in 10 mL of 0.05 M CF_3SO_3H . The resulting solution was loaded onto a Sephadex Spc-25 cation-exchange resin. By eluting with 0.2 M CF_3SO_3H and examining the UV-vis spectra of the solution 1.1×10^{-6} mol of $trans\text{-}[Ru^{IV}(TMC)O(OH_2)]^{2+}$ was found to be present.

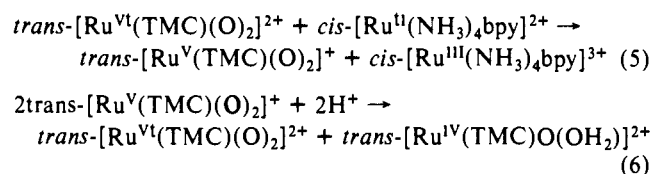
Results

In the presence of excess $trans\text{-}[Ru^{VI}(TMC)(O)_2]^{2+}$ in aqueous acidic medium, $cis\text{-}[Ru^{II}(NH_3)_4bpy]^{2+}$ is oxidized rapidly, as evidenced by the disappearance of its intense MLCT band at 522 nm (Figure 1a). Spectrophotometric titration indicated that 2 mol of Ru(II) were oxidized for each mol of Ru(VI) reduced (see Experimental Section). The reduction of Ru(VI) was accompanied by the corresponding stoichiometric appearance of $trans\text{-}[Ru^{IV}(TMC)O(OH_2)]^{2+}$. The formulation of the Ru(IV) product as oxo-Ru(IV) rather than dihydroxyruthenium(IV) is also supported by our recent work, in which the structure of $trans\text{-}[Ru^{IV}(L)O(OH_2)]^{2+}$ ($L = 1,12\text{-dimethyl-3,4;9,10\text{-dibenzo-1,12-diaza-5,8-dioxacyclopentadecane}$) has been determined by X-ray crystallography.^{2h} Thus the overall reaction can be represented by the equation



Preliminary mixing of the reactants in the stopped-flow apparatus ($[Ru^{VI}] \approx 5 \times 10^{-4}$ M, $[Ru^{II}] \approx 5 \times 10^{-5}$ M, pH = 1, $T = 298$ K) indicated that the reaction occurs in two stages. At 300 nm, near the λ_{max} of $trans\text{-}[Ru^V(TMC)(O)_2]^+$ (Figure 1b) and $cis\text{-}[Ru^{III}(NH_3)_4bpy]^{3+}$ a rapid first-order rise in absorbance was observed, which is followed by a slower second-order decay. At 522 nm, the λ_{max} of $cis\text{-}[Ru^{II}(NH_3)_4(bpy)]^{2+}$ a clean rapid first-order decay was observed which is in the same time scale as the rise in absorbance at 300 nm. On the basis of these and other evidences presented later, the two stages of the reaction can be represented by eqs 5 and 6 in Scheme I.

Scheme I



According to this scheme, the first stage of the reaction is the one-electron reduction of dioxoruthenium(VI) to dioxoruthenium(V), while the second stage involves the disproportionation of dioxoruthenium(V) to give dioxoruthenium(VI) and oxoruthenium(IV). The kinetics of these two steps are described separately below.

Kinetics of the Reduction of Dioxoruthenium(VI) to Dioxoruthenium(V). The kinetics were followed by measuring the disappearance of $cis\text{-}[Ru^{II}(NH_3)_4bpy]^{2+}$ at 522 nm. In the presence of at least a 10-fold excess of $trans\text{-}[Ru^{VI}(TMC)(O)_2]^{2+}$, clean pseudo-first-order kinetics were observed. The pseudo-first-order rate constants, k_{obs} , were obtained by nonlinear least-square fits of A_t to time t according to the equation $A_t =$

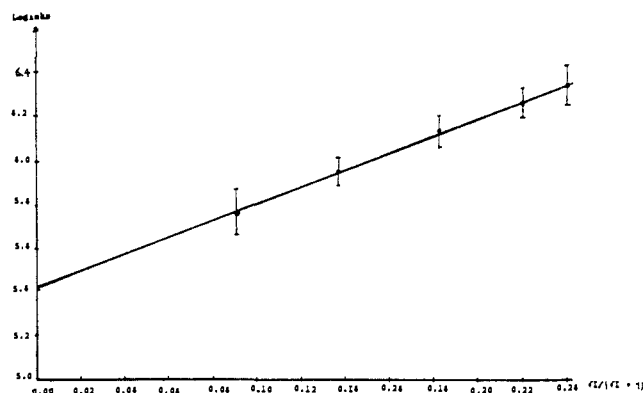


Figure 3. Plot of $\log k_2$ vs $\sqrt{I}/(\sqrt{I} + 1)$ for the reduction of $trans\text{-}[Ru^{VI}(TMC)(O)_2]^{2+}$ by $cis\text{-}[Ru^{II}(NH_3)_4bpy]^{2+}$ at 292.7 K.

Table I. Representative Second-Order Rate Constants for the Reaction $trans\text{-}[Ru^{VI}(TMC)(O)_2]^{2+} + cis\text{-}[Ru^{II}(NH_3)_4bpy]^{2+} \rightarrow trans\text{-}[Ru^V(TMC)(O)_2]^+ + cis\text{-}[Ru^{III}(NH_3)_4bpy]^{3+}$

T , K	I , M	$10^{-5} k_2$, $M^{-1} s^{-1}$
279.6	0.010	5.1 ± 0.3
286.4	0.010	5.6 ± 0.3
292.7	0.010	5.8 ± 0.3
	0.025	9.1 ± 0.5
	0.050	13.9 ± 0.8
	0.080	18.5 ± 1.0
	0.100	22.6 ± 1.3
298.0	0.010	6.1 ± 0.3
	0.100	24.2 ± 1.4
304.8	0.010	6.6 ± 0.4
310.6	0.010	7.1 ± 0.4
320.7	0.010	7.7 ± 0.4

^apH = 2.2, $[Ru^{VI}] = 5 \times 10^{-5}$ – 5×10^{-4} M, $[Ru^{II}] = 5 \times 10^{-5}$ – 5×10^{-6} M. ^b I = ionic strength.

$A_\infty + (A_0 - A_\infty) \exp(-k_{obs}t)$. A typical fit is shown in Figure 2. The pseudo-first-order rate constants were found to depend linearly on $[Ru^{VI}]$. Thus the experimentally determined rate law is

$$\frac{-d[Ru^{II}]}{dt} = k_2[Ru^{VI}][Ru^{II}] = k_{obs}[Ru^{II}] \quad (7)$$

Second-order rate constants, k_2 , obtained from linear least-squares fits of k_{obs} to $[Ru^{VI}]$, are independent of pH from 1.0 to 4.0.

The effect of ionic strength was investigated from 0.01 to 0.1 M at 292.7 K. Plot of $\log k_2$ vs $\sqrt{I}/(1 + \sqrt{I})$ is linear as shown in Figure 3. The observed slope of 3.98 is close to 4.08, the theoretical value given by the Debye-Huckel equation for a bimolecular reaction between two dications.

The activation parameters $\Delta H^\ddagger = (4.84 \pm 0.20)$ kJ mol⁻¹ and $\Delta S^\ddagger = -(117 \pm 20)$ J mol⁻¹ K⁻¹ ($I = 0.01$ M) were calculated by a least-squares treatment of $\log k_2/T$ vs $1/T$.

Representative kinetic data are collected in Table I. The kinetics of the reduction of Ru(VI) were also studied by using $[Ru^{II}(NH_3)_5isn]^{2+}$ and $[Ru^{II}(NH_3)_5py]^{2+}$ as reductants. Second-order rate constants at 25.0 °C are 3.0×10^6 M⁻¹ s⁻¹ ($I = 0.1$ M) and 3.4×10^6 M⁻¹ s⁻¹ ($I = 0.01$ M),¹⁵ respectively.

Kinetics of Disproportionation of Dioxoruthenium(V). The kinetics were followed at 300 nm corresponding to the disappearance of Ru(V) (which is produced in situ from Ru(VI) and Ru(II)). Visual inspection suggested that the decay curve is a hyperbola rather than an exponential function. A least-squares treatment of t/p (p = fraction of unreacted Ru(V), t = time) against t yielded a straight line with slope = 1, confirming a second-order kinetics (see Experimental Section). Thus the experimentally determined rate law is

$$\frac{-d[Ru(V)]}{dt} = k_{dis}[Ru(V)]^2 \quad (8)$$

Second-order rate constants, k_{dis} , were obtained by nonlinear least-squares fits of absorbance A_t to time t according to eq 3. A typical fit is shown in Figure 4. The pH dependence of the

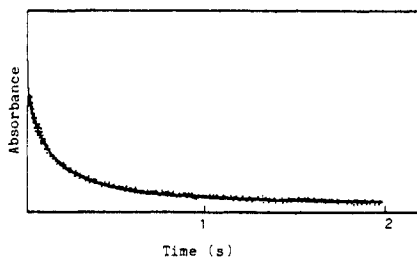


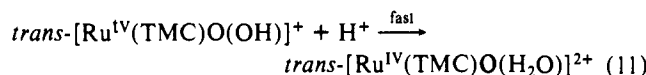
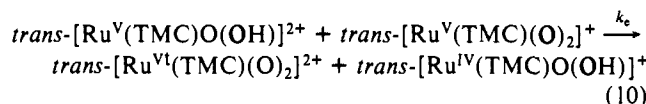
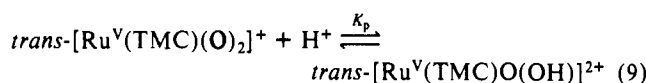
Figure 4. Typical absorbance vs time output of the nonlinear least-squares program for the disproportionation of $trans\text{-}[\text{Ru}^{\text{V}}(\text{TMC})(\text{O})_2]^+$ (5×10^{-4} M) at 300 nm, $T = 299$ K, $\text{pH} = 1.0$, and $I = 0.10$ M: dotted line, experimental data; solid line, theoretical curve.

Table II. pH Dependence of the Disproportionation of $trans\text{-}[\text{Ru}^{\text{V}}(\text{TMC})(\text{O})_2]^+$ at $T = 299$ K and Ionic Strength (I) = 0.10 M

$10^4[\text{Ru}(\text{NH}_3)_4\text{bpy}^{2+}]$, M	$10^3[\text{Ru}(\text{TMC})\text{O}_2^{2+}]$, M	pH	$10^{-3} k_{\text{dis}}$, $\text{M}^{-1} \text{s}^{-1}$
2.07	1.02	5.50	6.2 ± 0.3
1.10	0.61	5.00	12.2 ± 0.6
0.72	0.38	4.50	58 ± 4
0.96	0.50	4.00	188 ± 10
0.77	0.41	3.40	529 ± 30
0.51	0.30	3.00	540 ± 30
0.35	0.30	2.50	720 ± 40
0.60	0.33	2.00	341 ± 18
0.55	0.30	1.50	96 ± 6
0.57	0.35	1.00	39 ± 2

rate constant was studied in the range of 1–5.5 at 299 K and at an ionic strength of 0.1 M, and the results are summarized in Table II. A plot of k_{dis} vs pH gives a bell-shaped curve, as shown in Figure 5. These results are consistent with the following mechanism (Scheme II).

Scheme II



On the basis of this reaction scheme, it can readily be shown that

$$k_{\text{dis}} = \frac{2k_e K_p [\text{H}^+]}{(1 + K_p [\text{H}^+])^2} \quad (12)$$

A nonlinear least-squares analysis¹³ of the data in terms of eq 12 leads to $k_e = (2.72 \pm 0.34) \times 10^6 \text{ M}^{-1} \text{ s}^{-1}$ and $K_p = 615 \pm 50 \text{ M}^{-1}$ at 299 K.

The temperature dependences of k_e and K_p are summarized in Table III. The activation parameters $\Delta H^\ddagger = (18.7 \pm 2.9) \text{ kJ mol}^{-1}$ and $\Delta S^\ddagger = -(59.0 \pm 10.0) \text{ J mol}^{-1} \text{ K}^{-1}$ were calculated from a least squares treatment of $\ln(k_e/T)$ vs $1/T$.

Several runs were also made by using $[\text{Ru}^{\text{II}}(\text{NH}_3)_5\text{isen}]^{2+}$ as reductant to generate $[\text{Ru}^{\text{V}}(\text{TMC})(\text{O})_2]^+$. At 299 K and $I = 0.1$ M, k_{dis} was found to be $(37.9 \pm 1.8) \times 10^3$ and $(6.1 \pm 0.1) \times 10^3 \text{ M}^{-1} \text{ s}^{-1}$ at pH 1.0 and 5.5, respectively. The values of $k_e = (2.7 \pm 0.4) \times 10^6 \text{ M}^{-1} \text{ s}^{-1}$ and $K_p = 711 \pm 114$ are in satisfactory agreement with the values $k_e = (2.7 \pm 0.5) \times 10^6 \text{ M}^{-1} \text{ s}^{-1}$ and $K_p = 615 \pm 50$ obtained by using $cis\text{-}[\text{Ru}^{\text{II}}(\text{NH}_3)_4\text{bpy}]^{2+}$ as reductant.

Discussion

Reduction of Ru(VI) to Ru(V). The visible spectrum of $trans\text{-}[\text{Ru}^{\text{VI}}(\text{TMC})(\text{O})_2]^{2+}$ remains unchanged in acid solutions

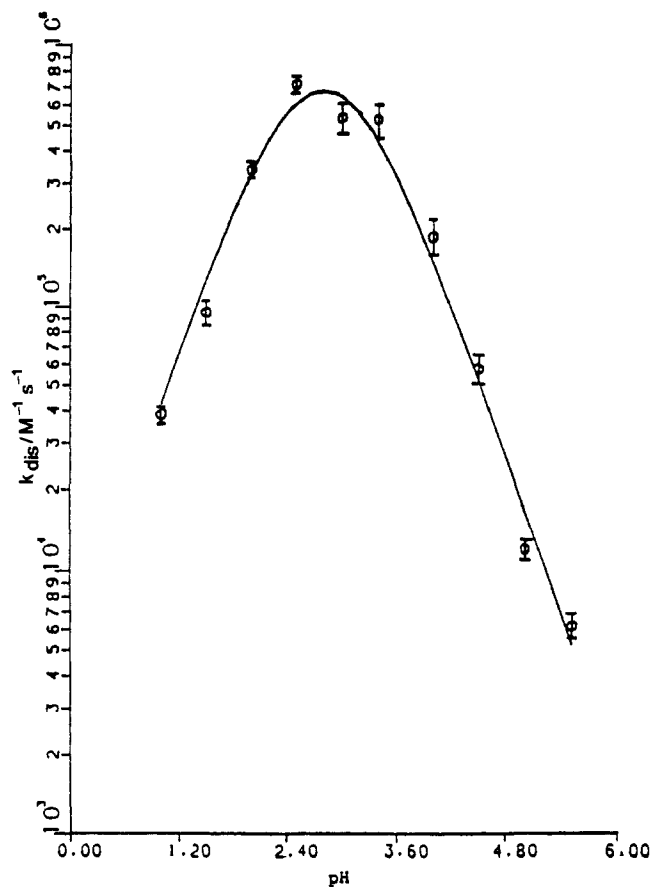


Figure 5. Plot of k_{dis} vs pH for the disproportionation of $trans\text{-}[\text{Ru}^{\text{V}}(\text{TMC})(\text{O})_2]^+$ at 299 K and $I = 0.10$ M.

up to 8 M, thus implying that the $\text{p}K_a$ of $trans\text{-}[\text{Ru}^{\text{VI}}(\text{TMC})\text{O}(\text{OH})]^{3+}$ is < -1 . This together with the pH independence of the reaction rate suggests that a pathway involving protonated Ru(VI) species is negligible in the pH range of 1–4 used in this study. The activation parameters for the reduction of $trans\text{-}[\text{Ru}^{\text{VI}}(\text{TMC})(\text{O})_2]^{2+}$ by $cis\text{-}[\text{Ru}^{\text{II}}(\text{NH}_3)_4\text{bpy}]^{2+}$ are of interest. The activation enthalpy for reaction 5 is quite small (4.84 kJ mol^{-1} at $I = 0.01$ M). It is thus unlikely that the reaction involves atom transfer where the activation enthalpy is usually much higher.^{2k} The data are consistent with an electron-transfer pathway.^{16–19} Given the substitution inertness and the structure of the reactants, it is unlikely to have an inner-sphere pathway for reaction. Thus the mechanism for the reduction of Ru(VI) to Ru(V) is likely to be outer-sphere in nature. In fact, the activation entropy for reaction 5 is also very close to the value of other known outer-sphere systems of the same charge composition.^{18,19}

Self-Exchange Rate of Ru(VI)/Ru(V). Assuming a simple outer-sphere mechanism, values for the self-exchange rate constant of the Ru(VI)/Ru(V) couple can then be estimated by the well-known Marcus–Cross relation.¹⁶

$$k_{12} = (k_{11}k_{22}K_{12}f_{12})^{1/2} \quad (13)$$

where

$$\ln f_{12} = \frac{(\log K_{12})^2}{4 \ln(k_{11}k_{12}/z^2)} \quad (14)$$

(15) The reaction between Ru(VI) and $[\text{Ru}^{\text{II}}(\text{NH}_3)_5\text{py}]^{2+}$ is too fast to be followed at $I = 0.1$ M.

(16) (a) Marcus, R. A. *J. Chem. Phys.* **1965**, *43*, 679, 2654. (b) Sutin, N. *Acc. Chem. Res.* **1982**, *15*, 275.

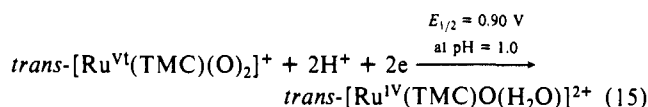
(17) Poon, C. K.; Tang, T. W. *Inorg. Chem.* **1984**, *23*, 2130.

(18) Brown, G. B.; Krentzien, H. Z.; Abe, M.; Taube, H. *Inorg. Chem.* **1979**, *18*, 3374.

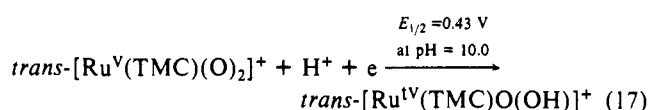
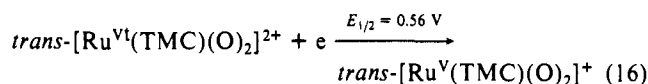
(19) Brown, G. M.; Sutin, N. *J. Am. Chem. Soc.* **1979**, *101*, 883.

In these equations k_{12} is the observed rate constant of the redox reaction, and k_{11} and k_{22} are the self-exchange rate constants for the component couples [here subscript "1" will refer to Ru(II) and subscript "2" to Ru(VI)]. K_{12} is the equilibrium constant for the reaction. z , a collision frequency, is taken as $10^{11} \text{ mol}^{-1} \text{ dm}^3 \text{ s}^{-1}$. The results of the Marcus calculations are summarized in Table IV. The three estimated self-exchange rate constants lie within an order of magnitude. The value obtained from *cis*-[Ru^{II}(NH₃)₄bpy]²⁺ is probably less reliable since the driving force in this case is very small ($\Delta E \approx 0.04 \text{ V}$) and hence a slight uncertainty in E could result in a large error in the calculated self-exchange rate. Hence we feel that the best estimate of the *trans*-[Ru(TMC)O₂]^{2+/1+} self-exchange rate constant is around $1.5 \times 10^5 \text{ M}^{-1} \text{ s}^{-1}$ (at 298 K and $I = 0.1 \text{ M}$). To our knowledge, there has been no prior self-exchange rate data for Ru(VI)/Ru(V) couples. This rate constant is similar to those of Ru(III)/Ru(II) couples: for example, *trans*-[Ru(14aneN₄)Cl₂]⁺⁰, 3.0×10^7 ($I = 0.5 \text{ M}$);¹⁷ [Ru(NH₃)₅(py)]^{3+/2+}, 4.7×10^5 ($I = 1.0 \text{ M}$);¹⁸ *cis*-[Ru(NH₃)₄(bpy)]^{3+/2+}, $7.7 \times 10^5 \text{ M}^{-1} \text{ s}^{-1}$ ($I = 0.1 \text{ M}$),¹⁹ where electron transfer occurs within the d_x orbitals. The large Ru(V)-Ru(V) self-exchange rate reveals a low inner-sphere reorganization energy for the electron-transfer reaction, as in the cases of [Ru^{II}(NH₃)₅py]²⁺ and *cis*-[Ru^{II}(NH₃)₄py]²⁺.^{18,19} This suggests that reduction of Ru(VI) to Ru(V) should not cause a significant distortion of the Ru=O and Ru-N(TMC) bonds. Previous X-ray structural works also established that the variations in the Ru-N (equatorial amine) and Ru=O distances from ruthenium(VI)-oxo to Ru(IV)-oxo complexes of macrocyclic tertiary amines are very small,^{2a,b,f} in accordance with the kinetic results described here.

Disproportionation of Ru(V). Evidence for disproportionation of Ru(V) first from cyclic voltammetric works.^{2d,8} In aqueous solutions having pH values between 1 and 7, *trans*-[Ru^{VI}(TMC)O₂]²⁺ exhibits a reversible two-proton two-electron Ru(VI)/Ru(IV) couple (eq 15), suggesting that the intermediate Ru(V) state is unstable with respect to disproportionation.



At pH > 7, the single two-electron wave begins to split into two waves which are assigned to half reactions (16) and (17).



The driving force for the disproportionation reaction (eq 6) can be obtained from eqs 15 and 16; at 298 K, pH = 1.0 and $I = 0.1 \text{ M}$, ΔG is equal to $-15.7 \text{ kcal mol}^{-1}$ ($K_{\text{disp}} = 3.2 \times 10^{11}$). This driving force decreases with increasing pH until at pH ≈ 7.3 , $\Delta G = 0$.

In nonaqueous medium *trans*-[Ru^V(TMC)O₂]⁺ is much more stable and can be readily isolated by electrochemical reduction of *trans*-[Ru^{VI}(TMC)O₂]²⁺.^{2d} Study of its disproportionation⁸ establishes the stoichiometry shown in eq 6. Direct kinetics study using the Ru(V) complex²⁰ proved to be difficult since the reaction is rather rapid even at high pH. The use of 1-e outer-sphere Ru(II) complexes, however, provides a convenient means of generating Ru(V) in situ from Ru(VI). The validity of this method is supported by its clean bimolecular kinetics and the independence of the subsequent disproportionation reaction rates to the reducing agent used.

From the pH dependence of k_{disp} , the disproportionation is shown to proceed via protonation of Ru(V) prior to electron transfer. The pK_a of *trans*-[Ru^V(TMC)O(OH)]⁺ is found to be 2.8 ($K_p = 615$ at 26.6 °C); thus on going from dioxoruthenium(VI) to dioxoruthenium(V), the pK_a of the protonated species increases by over 4 units.

Table III. Temperature Dependence for the Disproportionation Reaction of *trans*-[Ru^V(TMC)O₂]⁺ at $I = 0.10 \text{ M}$

$T, \text{ K}$	$10^6 k_e, \text{ M}^{-1} \text{ s}^{-1}$	$K_p, \text{ M}^{-1}$
299.0	2.72 ± 0.34	615 ± 50
304.7	3.41 ± 0.33	608 ± 60
	3.20 ± 0.32^a	1310 ± 130^a
310.6	3.75 ± 0.38	686 ± 60
320.7	4.95 ± 0.50	770 ± 93

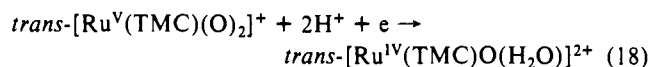
^aIn D₂O.

Table IV. Estimation of the *trans*-[Ru(TMC)O₂]^{2+/1+} ($E_{1/2} = 0.56 \text{ V}^a$) Self-Exchange Rate Constant at 298 K and $I = 0.1 \text{ M}$ from the Marcus-Cross Relation

reductant	$E_{1/2},^a \text{ V}$	$10^6 k_{12}, \text{ M}^{-1} \text{ s}^{-1}$	$10^5 k_{11}, \text{ M}^{-1} \text{ s}^{-1}$	$10^5 k_{22}, \text{ M}^{-1} \text{ s}^{-1}$
<i>cis</i> -[Ru ^{II} (NH ₃) ₄ bpy] ²⁺	0.52	2.4	7.7 ^b	15.0
[Ru ^{II} (NH ₃) ₅ isn] ²⁺	0.39	3.0	1.1 ^c	1.5
[Ru ^{II} (NH ₃) ₅ py] ²⁺	0.30	13.4	1.1 ^b	1.5

^aVs NHE. ^bReference 19. ^cThe exchange rate constant at 298 K and 1.0 M CF₃SO₃H is $4.75 \times 10^5 \text{ M}^{-1} \text{ s}^{-1}$ (ref 18); it is empirically corrected to $I = 0.1 \text{ M}$ by multiplying the rate constant at $I = 1.0 \text{ M}$ by 0.23 (see ref 19).

The $E_{1/2}$ value for the reduction of Ru(V) to Ru(IV) (eq 18) is 1.24 V at pH = 1 (from eqs 15 and 16).



Thus, in the presence of protons, Ru(V) is a more powerful oxidant than Ru(VI), and this provides the driving force for the disproportionation reaction.

The disproportionation rate constant, k_{disp} , exhibits apparently interesting solvent isotope effects. At pH (pD) = 1.0, $k_{\text{disp}}^{\text{D}} < k_{\text{disp}}^{\text{H}}$, but at pH (pD) = 4.5, the reverse is true. By calculating k_e and K_p from eq 12, it is found that $k_e(\text{H}_2\text{O})/k_e(\text{D}_2\text{O}) \approx 1$, while $K_p(\text{H}_2\text{O})/K_p(\text{D}_2\text{O}) = 0.46$ ($T = 304.7 \text{ K}$, $I = 0.1 \text{ M}$) (Table III). The lack of solvent isotope effect for k_e together with the substitution inertness of both reactants ([Ru^V(TMC)O₂]⁺ and [Ru^V(TMC)O(OH)]²⁺)²¹ are consistent with a simple outer-sphere electron-transfer mechanism.^{18,19,22} The observed solvent isotope effect on the equilibrium constant K_p is similar to that found in other oxo acid systems.²³

Self-Exchange Rate of *trans*-[Ru(TMC)O(OH)]^{2+/1+}. Assuming a simple outer-sphere mechanism, the self-exchange rate of *trans*-[Ru(TMC)O(OH)]^{2+/1+} can be estimated by using a value of $1 \times 10^5 \text{ M}^{-1} \text{ s}^{-1}$ discussed above for the self-exchange rate of *trans*-[Ru(TMC)O₂]^{2+/1+}. The $E_{1/2}$ for the *trans*-[Ru^V(TMC)O(OH)]^{2+/1+}/*trans*-[Ru^{IV}(TMC)O(OH)]⁺ couple is shown to be +0.80 V ($I = 0.1 \text{ M}$) using eqs 9 and 17. By entering these data into the Marcus-Cross relation, the self-exchange rate of *trans*-[Ru(TMC)O(OH)]^{2+/1+} is estimated to be around $5 \times 10^3 \text{ M}^{-1} \text{ s}^{-1}$. Like that of Ru(VI)/Ru(V), electron exchange between Ru(V) [(d_{xy})²(d_{xz})¹ configuration]^{2f} involves orbitals of n symmetry. The slower exchange rate of the Ru(V)/Ru(IV) couple is probably due to a larger Frank-Condon barrier associated with the conversion of a Ru^V=OH²¹ to Ru^{IV}-OH bond upon reduction.

Conclusion and Comments

[Ru^{VI}(TMC)O₂]²⁺ is unique among metal-oxo systems in two respects. First, electrochemically it exhibits a well-defined,

(20) The *trans*-[Ru^V(L)O₂](ClO₄)(L = 1,12-dimethyl-3,4,9,10-dibenzo-1,12-diaza-5,8-dioxacyclopentadecane) complex has recently been isolated and characterized by elemental analyses, IR spectroscopy, and magnetic susceptibility measurements. This Ru(V) complex is very stable in aqueous solutions having pH > 8. Preliminary kinetic studies showed that the reaction between *trans*-[Ru^V(L)O₂]⁺ and H⁺ is very similar to that of the disproportionation of *trans*-[Ru^V(TMC)O₂]⁺ described in this work. Tang, W. T. Ph.D. Thesis, University of Hong Kong, 1989.

(21) The Ru^V-OH bond should have partial double bond character and hence is expected to be inert to substitution.

(22) Weaver, M. J.; Nettles, S. M. *Inorg. Chem.* **1980**, *19*, 1641.

(23) Albery, W. J. In *Proton Transfer Reactions*; Caldin, E. F., Gold, V., Ed.; London: Chapman and Hall, 1975; p 263.

reversible Ru(VI)/Ru(IV) couple in acidic solutions as well as reversible Ru(VI)/Ru(V) and Ru(V)/Ru(IV) couples in basic solutions. Thus accurate redox potentials for these couples can be obtained. Second, the stability and rigidity imposed by the TMC ligand ensures that the complex and its reduced products persist in solution, thus giving rise to clean behavior. These factors together account for the detailed kinetics, thermodynamic, and mechanistic information that can be obtained in this study. Such information, apart from improving our understanding of high-valent ruthenium-oxo chemistry, would also help in the designing of efficient and selective ruthenium oxidants.

Electrochemical studies on other *trans*-dioxoruthenium(VI) species such as *trans*-[Ru^{VI}(bpy)₂O₂]²⁺,²⁰ indicated that their behavior is very similar to that of *trans*-[Ru^{VI}(TMC)O₂]²⁺. It seems that the disproportionation mechanism that we established in this study is a general one for the *trans*-dioxoruthenium(V) species. Moreover, this work implies that other d³ metal-oxo systems should also be unstable, and disproportionation of an oxo-manganese(IV) porphyrin system has been postulated recently.²⁴

The observed large self-exchange rates of the Ru(VI)/(V) and Ru(V)/(IV) couples and rate of disproportionation of Ru(V) suggest that the redox interconversion between Ru(VI) and Ru(IV) is rapid. This explains the reversibility of the two-electron Ru(VI)/(IV) couple observed in the electrochemistry of *trans*-dioxoruthenium(VI).

Acknowledgment. We thank the Croucher Foundation, the University and Polytechnic Granting Committee, and the University of Hong Kong for financial support.

Registry No. *trans*-[Ru^{VI}(TMC)(O)₂]²⁺, 95978-17-9; [Ru^{II}(NH₃)₄bpy]²⁺, 54194-87-5; [Ru^{II}(NH₃)₅isn]²⁺, 19471-53-5; [Ru^{II}(NH₃)₅py]²⁺, 21360-09-8; *trans*-[Ru^V(TMC)(O)₂]⁺, 103056-17-3.

Supplementary Material Available: Figure S1 of the spectrophotometric titration of *trans*-[Ru^{VI}(TMC)(O)₂]²⁺ with *cis*-[Ru^{II}(NH₃)₄bpy]²⁺ at 522 nm (1 page). Ordering information is given on any current masthead page.

(24) Groves, J. T.; Stern, M. K. *J. Am. Chem. Soc.* 1987, 109, 3812.

Polynuclear ((Diphenylphosphino)methyl)phenylarsine Bridged Complexes of Gold(I). Bent Chains of Gold(I) and a Role for Au(I)–Au(I) Interactions in Guiding a Reaction

Alan L. Balch,* Ella Y. Fung, and Marilyn M. Olmstead

Contribution from the Department of Chemistry, University of California, Davis, California 95616. Received February 5, 1990

Abstract: The role of weak Au(I)–Au(I) interactions in determining the structure and reactivity of a set of new, ligand-bridged complexes is described. Addition of 2 equivs of Me₂SAuCl to dpma [dpma is bis((diphenylphosphino)methyl)phenylarsine] yields Au₂Cl₂(μ-dpma) which has its two gold ions widely separated (7.011 (1) Å) but which packs about a center of symmetry so that there are two close (3.141 (1) Å) Au–Au contacts between molecules. ³¹P NMR spectra indicate that this molecule self associates at low temperature in solution also. Treatment of Au₂Cl₂(μ-dpma) with further Me₂SAuCl produces Au₃Cl₃(μ-dpma) which has a bent Au₃ chain (Au–Au distances 3.131 (1), 3.138 (1) Å; Au–Au–Au angle, 110.9 (1)°). The reaction of Au₂Cl₂(μ-dpma) with ammonium hexafluorophosphate or thallium nitrate yields [Au₄Cl₂(μ-dpma)₂][PF₆]₂ or [Au₄Cl₂(μ-dpma)₂][NO₃]₂, respectively. These have bent Au₄ chains (Au–Au distances 2.965 (1), 3.096 (1); Au–Au–Au angle, 88.0 (1)° in the hexafluorophosphate salt) with terminal P–Au–Cl groups and the dpma ligands aligned so that phosphorus is trans to arsenic on the central two gold ions. Comparisons of the solid state, associated form of Au₂Cl₂(μ-dpma) and [Au₄Cl₂(μ-dpma)₂]²⁺ suggest that the initial stage of formation of the Au₄ chain involves association of the Au₂Cl₂(μ-dpma) units through Au–Au interactions, despite the presence of vacant coordination sites on the gold ions and lone pairs on the arsenic atoms. The role of empty p acceptor orbitals on gold favoring the bent chains is developed.

Recent work on molecular recognition has focused attention on bonding interactions between molecules which are generally weaker than normal covalent bonds.¹ Among these are hydrogen bonds, electron donor/acceptor interactions and van der Waal's forces. The attractive interaction between Au(I) centers is another such interaction which, while weak, has important effects in determining molecular conformations and packing within gold(I) complexes.² It has been suggested³ that Au/Au contacts shorter than 3.5 Å are otherwise unexpected for such a large ion and it has been known that short Au–Au contacts (as short as 2.776 Å)⁴ are frequently seen in the solid state.³ Only recently, however,

has it been possible to estimate the energy associated with such bonds. Schmidbaur and co-workers have estimated that a Au–Au interaction (with a bond distance of 3.000 Å) has a bond energy of 7–8 kcal mol⁻¹.⁵

Most of the observed Au–Au interactions in Au(I) compounds involve pairs of gold ions,⁶ but a few examples of extended Au–Au interactions involving three or more gold ions are known.⁴ Here we present new structural data that show the ability of Au–Au interactions to orient molecules in the solid state in a configuration which is suggestive of an intermediate that is suitable for a reaction observed in solution. These interactions result in the formation of bent groups of three or four gold(I) ions. For this we used a flexible ligand, bis((diphenylphosphino)methyl)phenylarsine (dpma), that places minimal constraints on the gold–gold separations. Previous work with this ligand has focused on the use

(1) Lehn, J.-M. *Angew. Chem., Int. Ed. Engl.* 1988, 27, 89. Cram, D. J. *Angew. Chem., Int. Ed. Engl.* 1986, 25, 1039. *Host Guest Chemistry*; Parts I–III, Vögtle, F., Weber, E., Eds.; *Top. Curr.* 1984, 1982, 1981, 121, 101, 98.

(2) Schmidbaur, H. *Angew. Chem., Int. Ed. Engl.* 1976, 15, 728. Schmidbaur, H.; Dash, K. C. *Adv. Inorg. Chem. Radiochem.* 1982, 25, 239. Puddephatt, R. J. *The Chemistry of Gold*; Elsevier: Amsterdam, 1978.

(3) Jones, P. G. *Gold Bull.* 1981, 14, 102; 1981, 14, 159; 1983, 16, 114; 1986, 19, 46.

(4) Inoguchi, Y.; Milewski-Mahrla, B.; Schmidbaur, H. *Chem. Ber.* 1982, 115, 3085.

(5) Schmidbaur, H.; Graf, W.; Müller, G. *Angew. Chem., Int. Ed. Engl.* 1988, 27, 417.

(6) Throughout, our discussion is restricted to d¹⁰ Au(I) species, and we specifically exclude more reduced gold clusters from consideration. For emphasis, structural drawings use solid lines for the gold–gold interactions.